

A New Type of Hybrid Fish-like Microrobot

Wei Zhang*

Engineering, Kagawa University, Takamatsu 761-0396, Japan

Shu-Xiang Guo

Engineering, Kagawa University, Takamatsu 761-0396, Japan
Harbin Engineering University, Harbin 150001, PRC

Kinji Asaka

Kansai Research Institute, AIST, Midorigaoka, Osaka 563-8577, Japan

Abstract: In order to develop a new type of fish-like microrobot with swimming, walking, and floating motions, in our past research, we developed a hybrid microrobot actuated by ionic conducting polymer film (ICPF) actuators. But the microrobot had some problems in walking and floating motions. In this paper, we propose a concept of hybrid microrobot (see Fig. 1). The microrobot is actuated by a pair of caudal fins, a base with legs and an array of artificial swim bladders. We have developed a prototype of the base with legs and one artificial swim bladder, respectively, and carried out experiments for evaluating their characteristics. Experimental results show the base with legs can realize walking speed of 6 mm/s and rotating speed of 7.1 degrees/s respectively, and the prototype of the artificial swim bladder has a maximum floatage of 2.6 mN. The experimental results also indicate that the microrobot has some advantages, such as walking motion with 2 degrees of freedom, the walking ability on rough surface (sand paper), the controllable floatage, *etc.* This kind of fish-like microrobot is expected for industrial and medical applications.

Keywords: Biomimetic locomotion, ionic conducting polymer film (ICPF) actuator, hybrid microrobot, underwater microrobot.

1 Introduction

Underwater robots have powerful applications in many fields, such as aquatic life observation, medical diagnosis and seabed exploration. But traditional screw propeller is limited in some fields because of the noise and the electromagnetic field. For the last two decades, biomimetic robots have been focused on. Many kinds of locomotion of creatures have been used on robots, such as swimming, walking, crawling and so on^[1~5]. With the development of the micro system technology, underwater microrobots have urgently been demanded. In the microrobot fields, smart materials (like ionic conducting polymer film (ICPF), piezoelectric elements, pneumatic actuator, shape memory alloy) pave the way for a great variety of microrobot design.

In the last decade, ICPF actuators have been widely researched. An ICPF actuator consists of a perfluorosulfonic acid membrane with chemically plated gold as electrodes on both sides. It bends by applying a low

voltage between the electrodes^[6~9]. The actuator is soft and works in water or a wet environment. The ICPF actuator has several advantages. It bends with low voltage (above 1 V). It bends silently, responds quickly and consumes little energy. Its density is near to water. The electromagnetic field of the ICPF actuator is practically undetectable. However, as an emerging technology, ICPF has some disadvantages, such as weak propulsion and lack of long-term stability.

ICPF actuators are used as artificial muscles to drive robots^[10,11]. Because of its fast response, the ICPF actuator is widely used in swimming microrobots as oscillating or undulation fins^[12~19]. ICPF actuators are also used for biped walking underwater robot^[16,20]. A kind of ICPF micro leg with 2-DOF has been developed in [21]. A ciliary motion based 8-legged walking microrobot has also been developed in [22, 23].

Towards a hybrid fish-like robot as shown in Fig. 1, we developed an underwater fish-like microrobot actuated by ICPF actuators in [24], as shown in Fig. 2. The microrobot is actuated by a pair of caudal fins and two legs. The caudal fins propel the body forward in swimming motion. The legs have two functions. When the frequencies of legs are over 0.3 Hz, the legs act as the walking propellers, and the microrobot is in walking

Manuscript received July 8, 2006; revised August 28, 2006.

*Corresponding author. *E-mail address:*

s04d506@stmail.eng.kagawa-u.ac.jp

motion. When the frequencies of legs are lower than 0.3 Hz, the legs act as the floatage adjuster. They electrolyze the water, and the bubbles adhere to the microrobot, so the floatage is changed. In this way, the microrobot is in floating motion. The microrobot is 10 mm in width and 45 mm in length. Experimental results showed that it had a swimming speed of 5.5 mm/s, walking speed of 1.4 mm/s and floating speed of 2.7 mm/s. But the microrobot had some disadvantages in walking and floating motions: 1) The walking motion was only of one DOF; 2) Moving on rough surface was still a big problem; 3) The supporter was not a contributor of moving; 4) The bubbles were tiny (less than 10 mm³) and could not be collected and were difficult to get rid of.

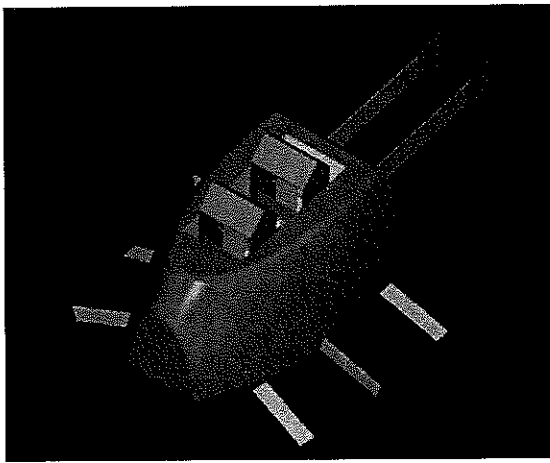


Fig. 1 A concept of hybrid fish-like underwater microrobot

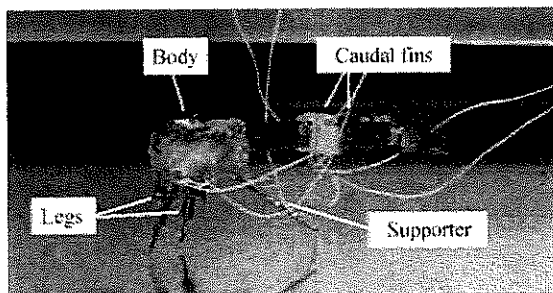


Fig. 2 A photo of the developed hybrid fish-like microrobot

In this paper, we propose a concept of hybrid fish-like microrobot. The microrobot consists of a pair of caudal fins, a base with legs and an array of artificial swim bladders, as shown in Fig. 1. The microrobot is proposed to have the following functions:

- 1) To have multi DOFs in walking motion;
- 2) To walk on rough surface;
- 3) To walk without resistance from the ground;
- 4) To collect the bubbles and attain a larger float-

age;

- 5) To release the bubbles freely.

This paper is structured as follows. Firstly, we introduce the concept of hybrid fish-like microrobot. Secondly, we introduce the moving mechanism of swimming, walking and floating motions. Thirdly, we develop the parts prototypes for walking motion and floating motion, and evaluate the characteristics. Lastly, we draw some conclusions.

2 A concept of hybrid microrobot

We propose a concept of a new type of hybrid fish-like microrobot. It consists of a body, a pair of caudal fins, a base with legs, and an array of artificial swim bladders, as shown in Fig. 3. The caudal fins generate the propulsion for swimming motion. The legs are used for walking. And the artificial swim bladders are the floatage adjuster.

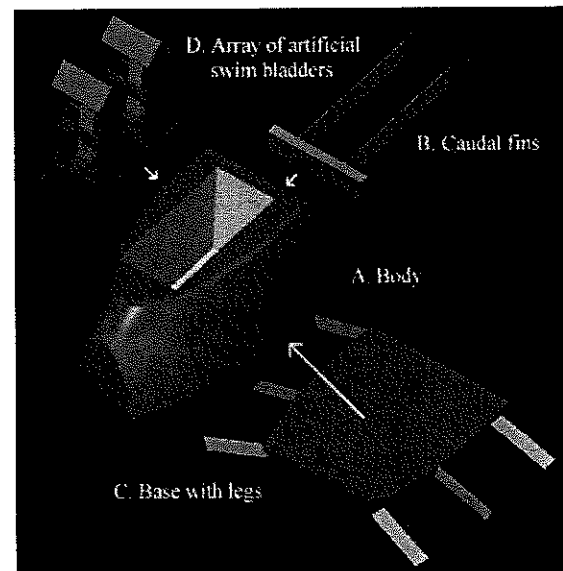


Fig. 3 The structure of the proposed microrobot

2.1 The structure of the base with legs

Insects are the experts in using legs. One step cycle of an abbreviated leg of the insect is shown in Fig. 4. Each step cycle can be divided into two phases, the swing-search phase and the stance phase^[25~27]. Traditional robots are always employing multi-joint legs inspired from nature. The multi-joint legs are flexible, but they need much space, actuators and complex control method and not suitable for microrobots.

We designed a structure with one-DOF actuators, as shown in Fig. 5-A-(a). The vertical actuator is called the driver. It is to offer moving propulsion. The horizontal actuator is the supporter and to lift

the driver up so that the driver can revert for the next propulsion. Supporters and drivers hold the body alternately^[28~30]. The strategies for some terrains are shown in Fig. 5. For a compact structure and the flexibility, based on our past work^[31,32], the base is developed using six actuators as shown in Fig. 6. The A, C and E are drivers, and the B, D, and F are supporters. Although they are asymmetric, adjusting the centers of drivers and supporters to the weight center, the asymmetric effect can be ignored.

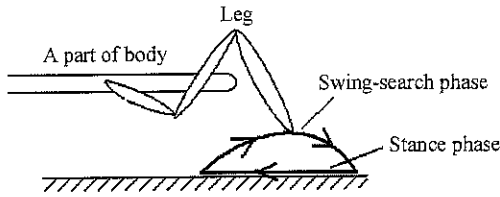


Fig. 4 The two main phases in insect walking (stick insect)

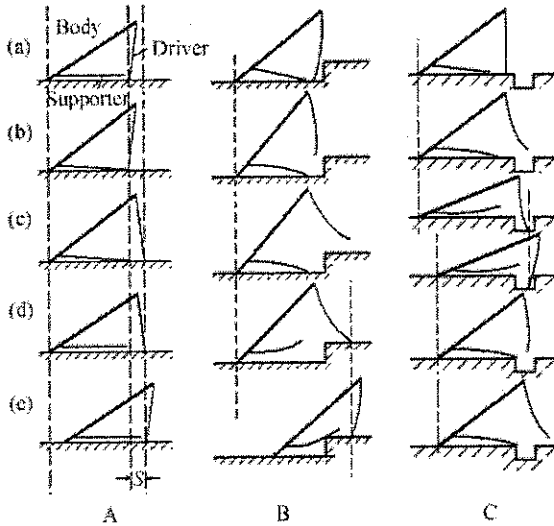


Fig. 5 Different strategies for different environments
A: Walking on flat surface, B: Climbing over a stair, C: Stride over a pit

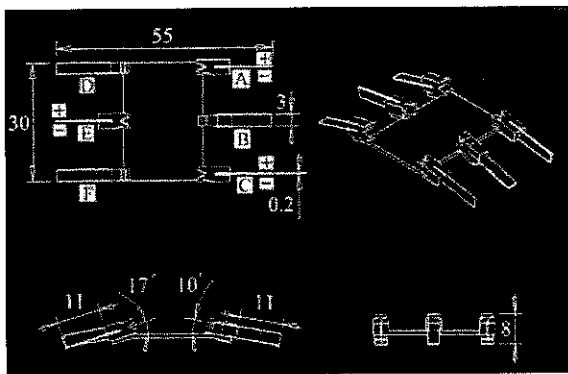


Fig. 6 The structure of the base with legs

2.2 The structure of the array of artificial swim bladders

The array of artificial swim bladders is inspired by the fish. It consists of several bladders, as shown in Fig. 7(b). One artificial swim bladder is shown in Fig. 7(a). It has one ICPF actuator to electrolyze the water to get the bubbles. A gas container is to collect the bubbles in its cavity, and it is conjoined to the base stander by a shaft so that it can rotate to release the bubble.

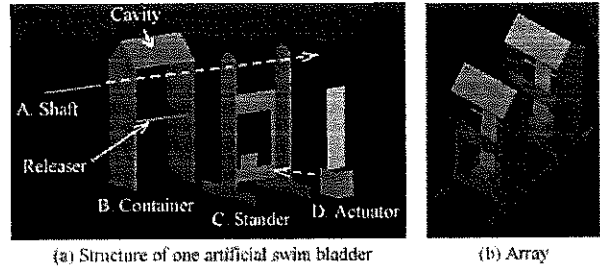


Fig. 7 The structure of the array of artificial swim bladder

3 The motion mechanisms of the micro-robot

3.1 The mechanism of the swimming motion

The caudal fins are two ICPFs offsetting with d , and driven by applied AC voltages as shown in Fig. 8. When proper phase difference appears, the fin generates an propulsion as shown in Fig. 9. Moving motions (forward, right turn and left turn) can be realized by changing frequencies of fins (as shown in Table 1).

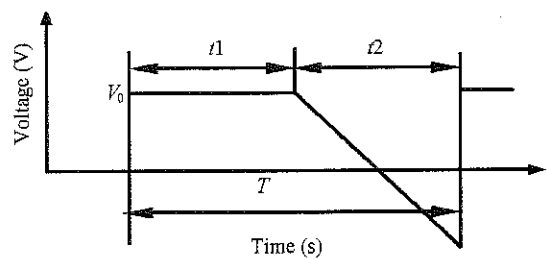


Fig. 8 Driving electric voltage for caudal fins

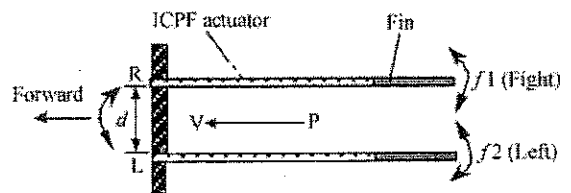


Fig. 9 Mechanism of the caudal fins

Table 1 The strategies of swimming motion

Motions	Conditions
Forward	$f1 = f2$
Right turn	$f1 > f2$
Left turn	$f1 < f2$

$f1$ and $f2$ stand for the frequencies of the caudal fins on right and left respectively

3.2 The mechanism of the walking motion

The drivers and supporters are in the same frequency, and the phase of supporters is delayed by 90 degrees, as shown in Fig. 10. The drivers offer the propulsion for walking. The supporters are not contributors of walking, but they help the drivers avoid the resistance from the ground when the drivers revert. Different walking motions can be realized, as shown in Table 2.

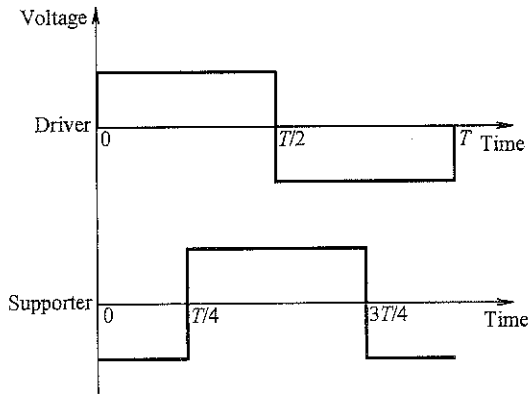


Fig. 10 The control signals of the base with legs

Table 2 The strategies of walking motion

Motions	A	C	E
Walking forward	-	-	-
Walking backward	+	+	+
Rotating in clockwise	+	+	-
Rotating in counter clockwise	-	-	+

A, C and E stand for the three drivers as shown in Fig. 6. “+” and “-” mean the drivers bending forward and backward respectively in stance phase

A step cycle of the fore-and-aft walking motion is separated into four periods. One step cycle in forward is shown in Fig. 11.

- 1) In period A ((d) to (a)), supporters lift the body up and drivers are lifted away from the ground.
- 2) In period B ((a) to (b)), drivers bend forward.
- 3) In period C ((b) to (c)), supporters bend upward enough so that supporters are away from the ground and drivers hold the ground.

4) In period D ((c) to (d)), drivers bend backward as the propulsion stroke, and the body is pushed forward.

During the swing-search phase (period A, B and C), drivers are away from the ground and find another foothold point with the help of supporters. In the stance phase (period D), drivers push the body forward.

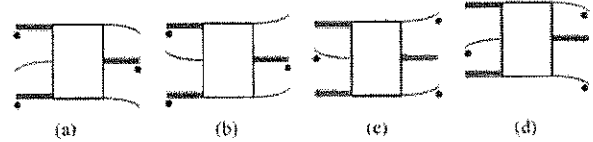


Fig. 11 One step cycle of moving forward (The marks ‘•’, indicate which legs contact the ground)

If the displacement of the actuator is d and the base with legs can move forward l in one step cycle, as shown in Fig. 12, then it is easy to obtain (1). And the speed is given by (2) where v is the average speed, and f stands for the frequency.

$$l = d \tag{1}$$

$$v = d \times f. \tag{2}$$

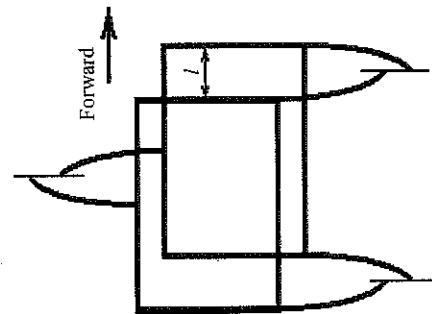


Fig. 12 The efficiency of the driver in walking motion (Supporters are not drawn out)

Rotating motion in counter-clockwise is shown in Fig. 13. As an abbreviated description, in the stance phase ((c) to (d)), drivers push the body rotating. In the swing-search phase, drivers prepare for the stroke with the help of supporters. The microrobot can rotate θ in one cycle described as (3), as shown in Fig. 14. From (4) and (5), θ can also be described as (6), where d is the displacement of drivers. And the rotating speed is (7), where ω and f stand for the rotating speed and the frequency respectively.

$$\theta = \pi + \alpha - 2\beta \tag{3}$$

$$\alpha = \alpha_1 + \alpha_2 = \arctan \frac{15 + d}{55} + \arctan \frac{15 - d}{55} \tag{4}$$

$$\beta = \frac{\pi}{2} + \alpha_2 = \frac{\pi}{2} + \arctan \frac{15 - d}{55} \tag{5}$$

$$\theta = \alpha_1 - \alpha_2 = \arctan \frac{15+d}{55} - \arctan \frac{15-d}{55} \quad (6)$$

$$\omega = \theta \times f = \left(\arctan \frac{15+d}{55} - \arctan \frac{15-d}{55} \right) f \quad (7)$$

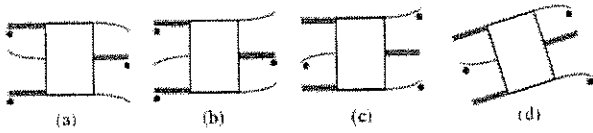


Fig. 13 One step cycle of the rotating motion (The marks '•', indicate which legs contact the ground)

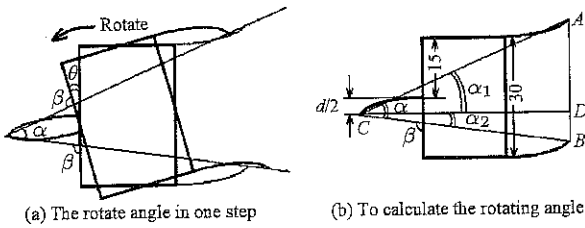


Fig. 14 The efficiency of the driver in rotating motion (Supporters are not drawn out)

3.3 The mechanism of the floating motion

The electrolyzing phenomenon of water proportions to voltage and inversely to frequency. When water around the ICPF surface is electrolyzed, the bubbles can change the floatage. We know that the floatage is

$$F = \rho \times V_a \quad (8)$$

where V_a , ρ and F are the microrobot volume, water density and floatage, respectively.

When the microrobot weight Mg is slightly larger than F , the microrobot is on the ground in water. When water is electrolyzed and the gas is collected by the gas container, the floatage is increasing, as shown in Fig. 15(a). The changing floatage, ΔF , is decided by the volume of the gas container, Δv , and the number of electrified artificial swim bladders, n , as shown in (9), where N is the total number of the artificial swim bladders.

$$\Delta F = n \times \Delta v \quad (n = 0, \dots, N). \quad (9)$$

When a higher voltage or lower frequency signal is applied to the actuator, the displacement of actuator is enlarged, so it drives the gas container rotating to expel the gas by pushing the releaser, as shown in Fig. 15(b).

In this case, the increasing floatage, ΔF , can be changed from 0 to $N \times \Delta v$, and the state of the microrobot in water can be controlled as shown in Table 3.

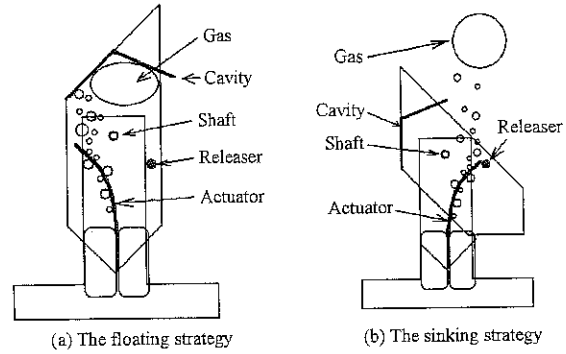


Fig. 15 The mechanism principle of the artificial swim bladder

Table 3 The strategies of floating motion

Motions	Conditions
Sink down until on the ground	$F + \Delta F < Mg$
Suspend in water	$F + \Delta F = Mg$
Float up until in the water surface	$F + \Delta F > Mg$

F and Mg are the floatage and weight of the microrobot respectively, and ΔF is the floatage increment of the artificial swim bladders

4 Characteristics and experimental results

4.1 The characteristic of the base with legs

We have developed a prototype of the base with legs as shown in Fig. 16. It is about 30 mm in length, 55 mm in width and 8 mm in height. The actuators are $11 \times 3 \text{ mm}^2$ and 0.2 mm in thickness.

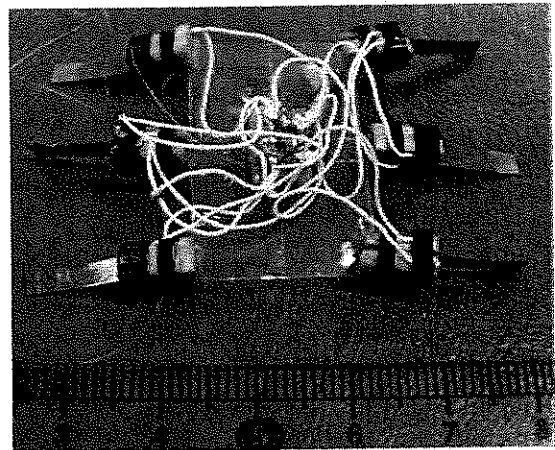


Fig. 16 The photo of the developed base with legs

Applying signals with different voltages and frequencies, we recorded the time for walking motion during 10 cm and rotating motion in 90 degrees. The calculated walking and rotating speeds are shown in Figs. 17 and 18. We also carried out experiment of climbing and striding. The base climbed on a 2 mm-high stair, and strode over a 5 mm-wide pit, with 0.5 Hz, 8 V.